

Mitigating Slow Dynamics of Low-Cost Chemical Sensors for Mobile Air Quality Monitoring Sensor Networks

Adrian Arfire, Ali Marjovi, and Alcherio Martinoli
Distributed Intelligent Systems and Algorithms Laboratory
School of Architecture, Civil and Environmental Engineering
École Polytechnique Fédérale de Lausanne, Lausanne, Switzerland
{firstname.lastname}@epfl.ch

Abstract

The last decade has seen a growing interest in air quality monitoring using networks of wireless low-cost sensor platforms. One of the unifying characteristics of chemical sensors typically used in real-world deployments is their slow response time. While the impact of sensor dynamics can largely be neglected when considering static scenarios, in mobile applications chemical sensor measurements should not be considered as point measurements (i.e. instantaneous in space and time). In this paper, we study the impact of sensor dynamics on measurement accuracy and locality through systematic experiments in the controlled environment of a wind tunnel. We then propose two methods for dealing with this problem: (i) reducing the effect of the sensor's slow dynamics by using an open active sampler, and (ii) estimating the underlying true signal using a sensor model and a deconvolution technique. We consider two performance metrics for evaluation: localization accuracy of specific field features and root mean squared error in field estimation. Finally, we show that the deconvolution technique results in consistent performance improvement for all the considered scenarios, and for both metrics, while the active sniffer design considered provides an advantage only for feature localization, particularly for the highest sensor movement speed.

Categories and Subject Descriptors

C.2.4 [Computer-Communication Networks]: Distributed Systems—*Distributed applications*; C.3 [Special-Purpose and Application-Based Systems]: Real-time and embedded systems

General Terms

Data processing, Experimentation, Design

Keywords

Mobile Wireless Sensor Networks, Air Quality Monitoring, Chemical Sensors

1 Introduction

In 2014, the World Health Organization singled out air pollution as the current largest environmental health risk, with more than 7 million deaths related to air pollution recorded in 2012 alone [31]. This number doubled previous estimates, and was justified by progress in understanding diseases caused by air pollution, but also by improved estimations of human exposure to pollution through the use of new measurement technologies.

Our ability to measure and predict air quality parameters at a spatial resolution relevant for human health is, however, still very limited. Most of the information we currently get on the state of air pollution comes from networks of large stationary monitoring stations. The measurement equipment employed in these networks delivers highly accurate data, but is typically very expensive, leading to a prohibitively high price for any significant scale-up. The resulting monitoring networks are very sparse (e.g., the Swiss National Air Pollution Monitoring Network - NABEL - uses a total of 16 stations for the whole country).

The low resolution of traditional monitoring networks limits our ability to capture the spatial heterogeneity of the air pollution field. This is particularly significant for urban settings, where the locality of emission sources (e.g., industries, traffic) and the specific urban landscape (e.g., street canyons, green areas etc.) lead to highly heterogeneous concentration levels.

Wireless Sensor Networks (WSNs) hold the potential to increase the currently achievable spatial density of measurements, and, over the past decade, there has been a growing interest in the development and deployment of such networks that use low-cost air quality sensors. While there are a few examples of static network deployments [5, 6], most projects have targeted hybrid (i.e. a mix of static and mobile sensor nodes), or fully mobile deployments. The main reason for choosing mobility stems from economical reasoning, as the deployment, maintenance and running costs for covering an entire city with a network of static nodes would still be impractically high.

In an urban scenario, there is a significant diversity of potential mobility sources ranging from pedestrians

and cyclists, to private vehicles and public transportation. Examples of projects that have used pedestrian mobility are MESSAGE [17], CitiSense [3], EveryAware [10], AIR [25], and Common Sense [8]. Bicycles have been used in the Copenhagen Wheel [28], and Aeroflex [9] projects. Finally, private cars were considered in the MAQUMON project [16], and public transportation in Citi-Sense-MOB [4], and our OpenSense project¹, within which two different sets of assets were developed and deployed on trams in Zurich [14] and on buses in Lausanne [23].

The growing interest in mobile WSNs for air quality monitoring is easily apparent from the number of projects mentioned above. However, the quantity of published results based on deployment data is still relatively low. While in the case of ultrafine particles (UFPs), significant results have been obtained in pollution mapping using mobile deployment data, by Hasenfratz et al [15], Li et al [19], and Marjovi et al [23], this has not been the case for gaseous pollutants. The main reason for this can be found in the significant challenge of ensuring data quality during the whole deployment period. Chemical sensors suffer from a list of problems that the electrical detection devices used for measuring ultrafine particles, in the aforementioned works, generally do not. This includes poor sensitivity, combined with high sensor noise (i.e. low signal-to-noise ratio), sensor instability requiring frequent re-calibration, and slow response times, which, in the context of mobility, leads to signal distortion. Dealing with all of these issues is a daunting task, and while some success has been achieved for some of them, there has been no significant work published so far on mitigating the problem of slow sensor dynamics.

1.1 Chemical Sensors

Technological advances in the field of chemical sensors have significantly increased the availability of small and cheap sensors for measuring various gas-phase species. Nevertheless, the data quality obtained from these sensors is significantly lower than that of traditional instrumentation (e.g., mass spectrometers).

The most commonly used chemical sensors for WSNs applications are either electrochemical or metal-oxide. Both classes of sensors suffer, although to different degrees, from temporal drift, cross-sensitivity, and temperature, humidity or pressure dependence [1, 29]. These issues imply that, even when factory calibration is available, regular re-calibration is necessary, in order to ensure a baseline of quality to the data. This problem needs to be handled through online calibration algorithms, since frequent manual offline re-calibration would be impractical for large scale deployments. Important results in this field are the works of Hasenfratz et al [13] and Saukh et al [27, 26]. Furthermore, in one of our previous works [2], we proposed a model-based rendezvous calibration technique and studied the benefit of increasing the complexity of the sensor model used by the algorithm.

Beyond calibration, dealing with the slow dynamics of chemical sensors in a mobile application is a key issue. Chemical sensors typically have long response times to stimuli, which can range from a few seconds to multiple

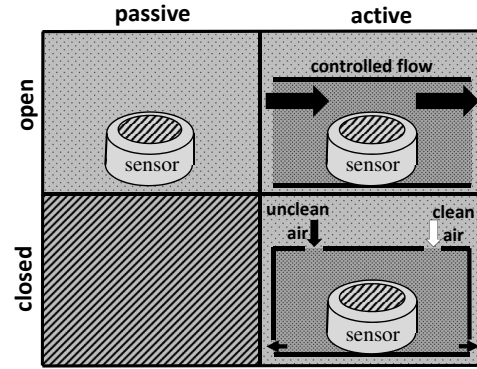


Figure 1. Classification of sampling system designs.

minutes. While for static deployments, this issue can be largely neglected, for mobile platforms it can induce significant distortion of the measured signal with respect to the underlying concentration levels.

Within the field of mobile WSNs, the slow-dynamics of chemical sensors has, unfortunately, so far gone unaddressed: most of the previously mentioned works assume measurements to be instantaneous. This problem has, nevertheless, been acknowledged in the field of mobile robot olfaction. Strategies for mitigating such effect include speed limitation of the robotic platforms [21], cycling between movement and stationary measurement behaviors [30], and the use of specially designed air sampling systems [18, 20, 22].

While the first two strategies cannot generally be considered in the case of mobile WSNs, which typically leverage parasitic mobility, the design of sampling systems needs to be investigated.

1.2 Air Sampling Systems

As represented in Figure 1, sampling system designs can be broadly classified in the following way:

- **Open passive samplers** are systems that rely only on naturally existing air flows and the relative flow induced by locomotion for transporting the target gas molecules towards the sensitive surface of the transducer. The advantage of this design rests in its simplicity and low-cost. Currently, most of the sensor nodes used in mobile WSNs applications fall in this category [3, 25, 8, 28, 16].
- **Open active samplers**, also known as active sniffers, employ devices like fans or vacuum pumps to draw and flush air around the sensor for improving its dynamic response. While this approach has been used in some projects [10, 15, 4], no results analyzing the effectiveness of the considered designs has been published to date.
- **Closed active samplers**, or closed chamber systems, are measurement systems in which a sample of air is drawn into a sensor chamber, usually with a pump. The chemical sensors are then exposed to this sample until their output signal stabilizes. Then the sampled air is expelled, by drawing from a source of clean

¹<http://opensense.epfl.ch>

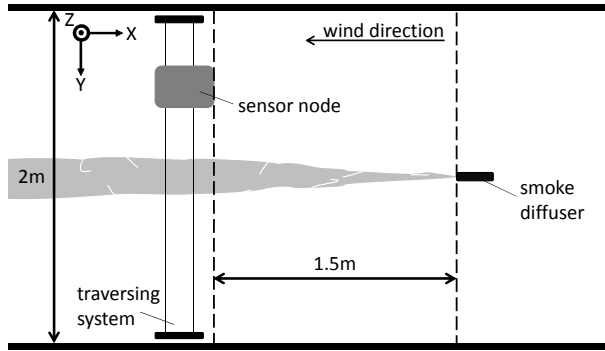


Figure 2. Top view of experimental set-up inside wind tunnel (not to scale).

air. The sensor is left to recover, after which the cycle restarts. The advantage of this type of system is that, differently from the two previous classes of samplers, it can provide absolute concentration levels. However, in order to achieve the desired stability inside the chamber, a practical implementation of this measurement principle needs to consider non-trivial aspects like the reactivity of the targeted gasses to each other, and to contact surfaces inside the chamber and on the air-flow path. Furthermore, such a system is relatively more complicated and less light-weight, making it less attractive for mobile WSNs applications. Finally, the time needed for a complete measurement cycle implies a low measurement frequency and leads to a problem of time budgeting. To the best of our knowledge, no closed-chamber sensor node designs currently exist for mobile WSNs applications.

1.3 Our Contribution

In this paper we study the impact of mobility on chemical sensing accuracy through a rigorous experimental framework. For this purpose, we make use of a mobile air sensing platform that we have developed within the OpenSense project, for a long term real-world deployment in the city of Lausanne, Switzerland.

We show that the effect of mobility is significant and that it has to be taken into account when working with chemical sensors for mobile air quality monitoring. We consider both passive and active open sampling systems and we propose to use a deconvolution technique for improving the quality of our measured signals.

To the best of our knowledge, none of the previous works has studied in detail this important problem. Moreover, the proposed solutions have never been evaluated through rigorous experimental trials.

2 Experimental Set-up

In order to isolate and investigate the effect of mobility on a chemical sensing platform, we designed a controlled experimental set-up. This task was in no way trivial, due to the stochastic nature of gas dispersion, and the difficulty of getting a ground-truth of the measured field.

We conducted all our experiments inside a wind tunnel,



Figure 3. One of our sensor nodes anchored to the roof of a Lausanne bus. The gas sampling system used in this paper is a sub-module of this real-world platform.

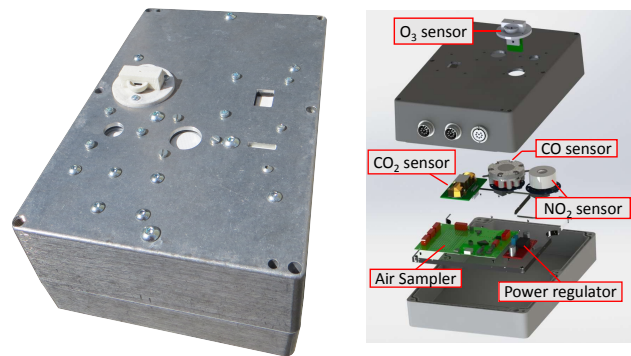


Figure 4. Closed (left) and exploded (right) views of the gas sampler box. In its standard form it is an open passive sampler.

and used a sensor node design which we have also extensively tested in a real-world deployment. The sensor node was attached to a traversing system (i.e. a cartesian coordinate robot), which allows varying the speed of the movement in a controlled and repeatable way. As a source of pollution, we used a smoke machine which created a chemical plume that our sensor node is able to detect. Figure 2 shows a schematic representation of our experimental set-up.

2.1 Mobile Sensor Node

The gas sampling system we used in our experiments is part of a modular mobile air quality monitoring platform that we developed and deployed on 10 buses of the Lausanne public transportation company (see Figure 3). Apart from this system, all the mobile sensor nodes in our deployment also include an ultrafine particle sampling module, a localization module, and a data-logging and wireless communication module. This represents a complete mobile air quality sensor node design, which measures carbon monoxide (CO), nitrogen dioxide (NO₂), ozone (O₃), carbon dioxide (CO₂), and particulate matter (PM). These constitute the most relevant urban air pollution parameters commonly monitored both in the U.S. [11], and the European

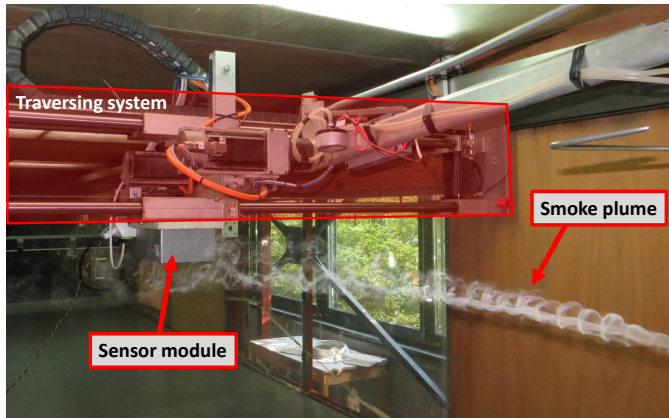


Figure 5. Sensor node traversing the smoke plume inside our wind tunnel.

Union [12]. Our mobile sensor network has been operational and successfully gathering data for more than 2 years to date.

For the purpose of this work we focused only on the gas sampling module, a self-contained system which measures the aforementioned gas-phase pollutants, and transmits the measured values over a CAN bus. The CAN data stream was logged using a standard desktop workstation which also controlled the motion of the traversing system, and the wind speed inside the tunnel.

In its standard form, the gas sampling module is an open passive sampling system (see Figure 4), but provisions have been taken in its design for it to be easily upgradeable to both open-active and closed-active forms (e.g., it is able to power and control multiple valves, pumps or fans).

Out of the list of available sensors we opted to focus on the City Technology A3CO carbon monoxide electrochemical sensor [7]. The reason for this choice is based on the high selectivity and relatively good temporal stability (i.e. low drift) of this sensor, which permit a better isolation of the problem targeted in this study.

2.2 Wind Tunnel

We performed our experiments in a boundary layer wind tunnel, with dimensions of $1.5 \times 2 \times 10 \text{ m}^3$, and a maximum wind speed of 24 m/s. The sensor box was attached with the sensors facing down (similar to our bus deployment), onto the tunnel's traversing system. During our experimental runs, we performed movements in the cross-wind direction (only the Y-axis of the traversing system), while locking all other axes (see Figures 2 and 5).

The working wind-speed for all the experiments presented in this paper was 0.5 m/s, which was selected through manual tuning as a tradeoff between the width of the smoke plume and its stability. We used the whole working length of the Y-axis which is 1.4 m (smaller than the actual width of the wind tunnel). In our experiments we varied the velocity of the traversing system incrementally from 2.5 cm/s, and up to 10 cm/s.

2.3 Chemical Plume Source

For generating a chemical plume we used the Pea Soup Wind Tunnel Air Flow Tracer SGS-90 [24], which produces

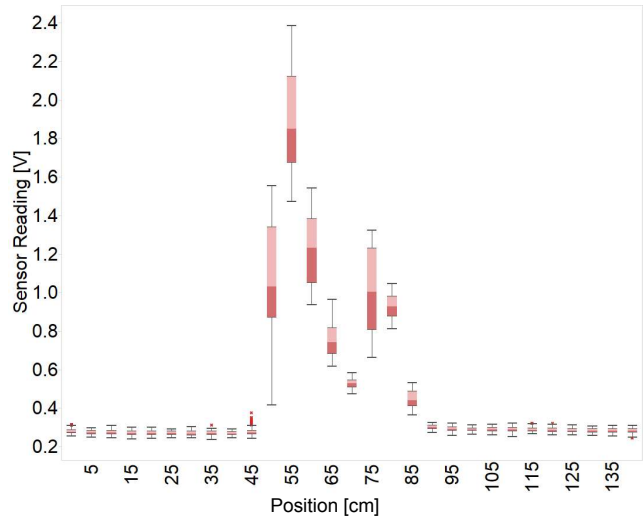


Figure 6. Cross-wind plume profile ground-truth estimation. The boxplots of the data acquired at each location illustrate the local distribution of the gas concentration. The structure of the plume was kept stable throughout all experiments.

smoke by heating a white mineral oil flowing through a diffuser. The quantity of smoke can be controlled by tuning the oil flow and heating voltage, and was set to be consistent over our different experiments. A great advantage when using a smoke machine as plume generator is that this permits a direct visualization of the shape and stability of the plume (see Figure 5).

In order to get a good estimation of the plume ground-truth, we designed and conducted the following experiment: we commanded the traversing system to move at regularly spaced positions on the Y-axis, with a 5 cm increment. At each of these positions 130 s of data were acquired (i.e. more than the manufacturer stated response time of maximum 40 s). We used a sampling period of 60 ms, which was kept constant also for the rest of the experimental work presented in this paper. After each interval of static data acquisition, the sensor was moved out of the plume (at the zero position), and left for 120 s to ensure its full recovery, before moving to the next 5 cm increment. The data was then processed by clipping the first 40 s of data for each position.

The resulting estimation of the plume profile is represented through a collection of boxplots in Figure 6. In this paper we assume the convention of extending boxplot whiskers up to 1.5 of the interquartile range. The resulting graph shows that, in spite of an important variability of the concentration level within the plume, our experimental set-up is able to maintain its overall structure and position. The distinct two-peak concentration profile is most probably due to the fact that, at the considered wind speed, the smoke diffuser induces a ring-like cross-section to the plume. This effect can be directly observed in the shape of the smoke in Figure 5.

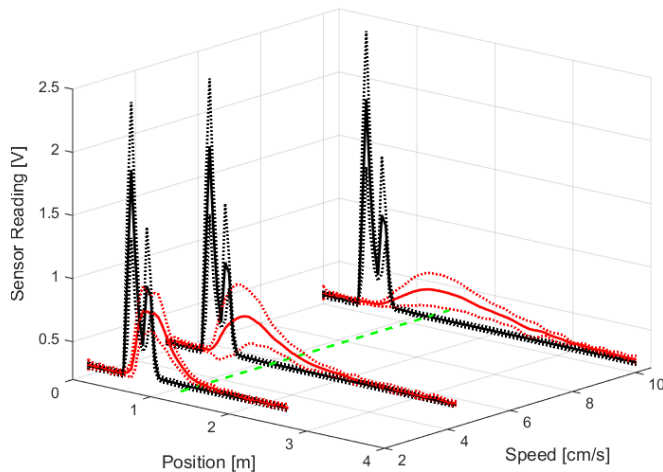


Figure 7. Average measured signal (red) over 10 runs at different speeds of the traversing system versus the reference plume profile (black). Dotted lines represent 2σ confidence intervals. The green dashed line marks the end of each run where the sensor node stops moving. For visual clarity, we unfold the data recorded at this position as if the movement would have continued with the same velocity.

3 Mitigating the Slow Sensor Dynamics

After obtaining a good estimate of the underlying signal, we proceeded with a series of repeated dynamic scans of the plume at several constant speeds. Once the sensor node reached the end of a run, we continued logging the data until the sensor recovered its baseline reading. We considered movement speeds of 2.5 cm/s, 5 cm/s and 10 cm/s, and performed 10 runs for each setting.

The results of this set of experiments are presented in Figure 7. These clearly show that, even for relatively low speeds of the sensor node, the signal distortion is significant. Due to its slow response time, the chemical sensor appears to perform largely as an integrator of the underlying signal over time, leading to a larger distortion when the speed of the node is increased.

The effect can be seen as analogous to motion-blurring in photography, which happens when the exposure time of a camera system is long relative to its movement speed. A typical signal processing approach for reducing the effect of motion-blurring is through deconvolution.

In the next subsection, we first consider a mechatronic approach for improving the dynamics of the chemical sensor: the use of an open active sampler. We then propose a deconvolution filter in order to estimate the true underlying signal.

3.1 Active Sniffing

In order to investigate the opportunity of using an active sniffer, we have developed and evaluated a simple design, using a small axial fan rated for an air-flow of up to $0.034 \text{ m}^3/\text{min}$. Since the benefit of active sniffing stems from the ability to increase air flow around the chemical

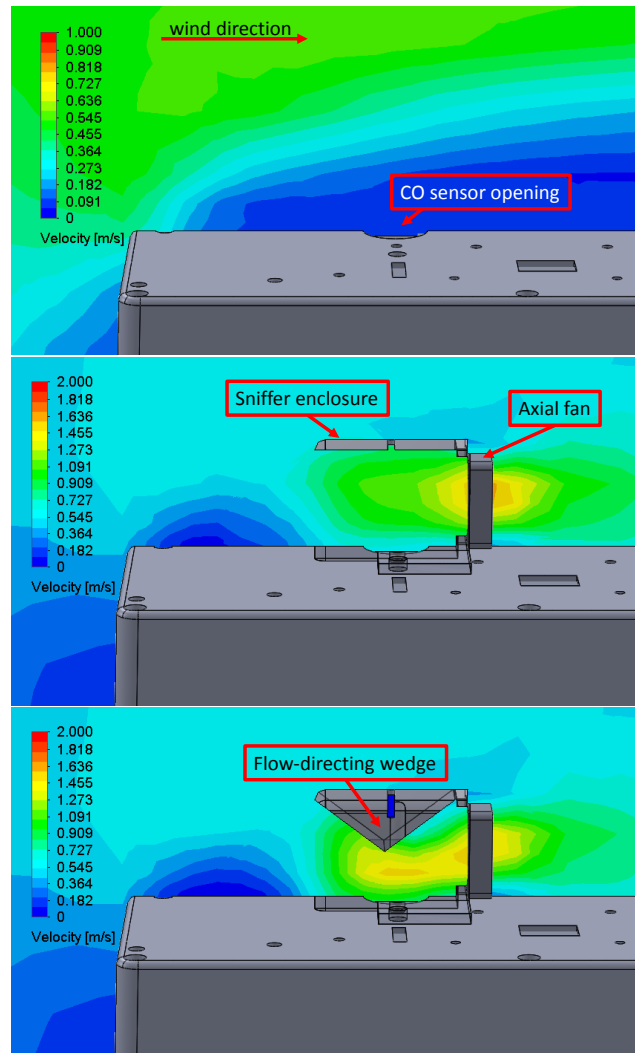


Figure 8. Main steps of active sniffer design: evaluation of velocity profile of the air flow for the open passive design (top), and for the active design without (middle) and with (bottom) flow-directing wedge. Because the air flow for the passive design is significantly lower, the maximum of the colormap was decreased, for visibility.

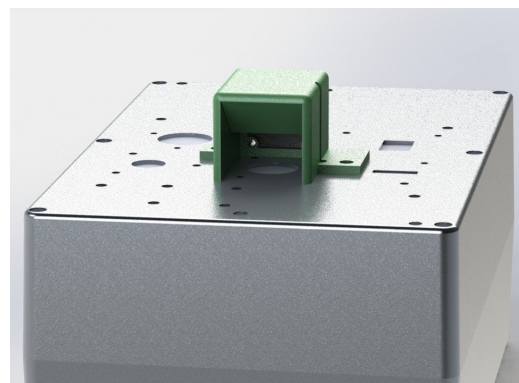


Figure 9. Final design of active sniffer, mounted above the CO sensor opening.

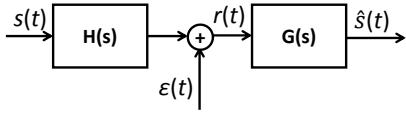


Figure 10. A deconvolution procedure convolves a distorted signal with a filter $G(s)$, in order to obtain an estimation of the original signal.

sensor, we made use of Computational Fluid Dynamics (CFD) simulations in the design process, to ensure that this goal is indeed achieved.

These were performed using an accurate 3D mechanical model of the sensor box and the SolidWorks Flow Simulation package. We considered a laminar background flow set to match the one used in the wind tunnel experiments (i.e. 0.5 m/s), and a simulation model of the axial fan was produced using the performance curve supplied by its manufacturer. The main steps of this design process are presented in Figure 8, which shows the velocity profile in a vertical plane, defined by the wind direction vector and the axis of symmetry of the chemical sensor.

Already the first step, of adding a small enclosure with a fan, significantly increases the air flow in the vicinity of the chemical sensor. The use of an additional down-pointing wedge-shaped feature on the interior of the enclosure helps in directing the flow towards the sensor, further increasing the air velocity close to its surface. An overview of the final CAD design of the sniffer can be seen in Figure 9. Based on this design, we 3D printed a sniffer prototype which we used in our subsequent experiments.

3.2 Deconvolution

We adopt the following formalism: Let $s(t)$ be the underlying carbon monoxide concentration level that we would like to measure, and $h(t)$ the impulse response of the electrochemical sensor we are using, and $S(s)$ and $H(s)$, their respective Laplace transforms. The sensor reading $r(t)$ can then be expressed as:

$$r(t) = (s * h)(t) + \varepsilon(t) \quad (1)$$

where the symbol $*$ denotes the convolution operation, and $\varepsilon(t)$ represents an additive noise signal.

The goal of a deconvolution algorithm is to find a filter $g(t)$ ($G(s)$ in frequency domain), which applied to the measured signal, can achieve a good estimation of the original signal:

$$\hat{s}(t) = (g * r)(t) \quad (2)$$

A schematic representation of the principle of deconvolution is shown in Figure 10.

Depending on the choice of the independent variable for our signals, the measurement distortion and deconvolution filter can be studied either through space, or through time. These approaches are equivalent as long as the sensor node moves at a constant speed. However, since this is not a valid hypothesis for real-world mobility, we opt to conduct our analysis of the signals as functions of time. This allows

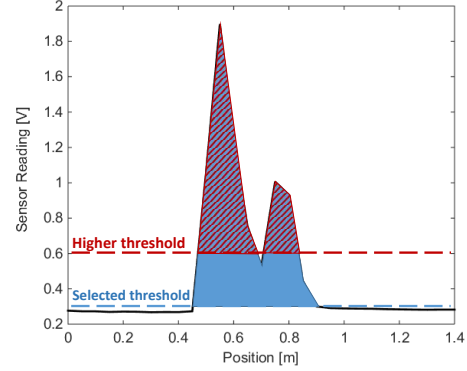


Figure 11. Threshold segmentation. The number of resulting features depends on the choice of threshold level. Our selected level (blue) generates a single feature, while a higher level of 600 mV (red), would generate two.

us to have a single model of the sensor’s distortion process, independent of changing velocities.

A popular method for performing deconvolution is through the use of the Wiener filter, which minimizes the mean squared error between the estimated and the desired signals. The Wiener deconvolution filter is most easily described by using the Fourier transform:

$$G(f) = \frac{H^*(f)}{|H(f)|^2 + 1/SNR(f)} \quad (3)$$

where the superscript $*$ symbol represents complex conjugation, $H(f)$ is the Fourier transform of $h(t)$, and $SNR(f)$ is the signal-to-noise ratio. In the ideal case, when noise is absent, the Wiener filter becomes the inverse of $H(f)$.

In order to use the Wiener filter, a model of the chemical sensor is required, and also an estimation of the noise present in the measured signal. We assume a second-order filter model for the chemical sensor, of the form:

$$H(s) = \frac{K}{(s + c_0)(s + c_1)} \quad (4)$$

where K is a constant parameter of the model, and c_0 and c_1 are its two poles. This model was selected, after multiple trials with other filter orders, as it provided a good balance between complexity and data-fitting performance.

We estimate the model parameters through system identification, by using the reference average plume profile as system input data, and the set of measured signals over the dynamic experiments as system output. The amount of noise present in the measurement process is estimated by using the sensor readings outside of the plume, where we assume that the variation of the sensor reading is caused only by additive noise.

4 Results

In evaluating the performance of our proposed methods for reducing the effect of the chemical sensor’s slow dynamics, we have used the following two metrics:

- **Feature localization accuracy** - This metric quantifies the ability of the system to estimate the position of

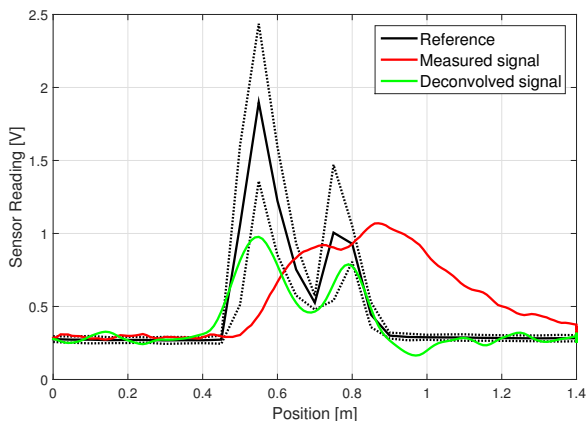


Figure 12. Signal deconvolution example. The measurement data was gathered using the active sniffer during a run at 2.5 cm/s. By using the Wiener deconvolution, for this experiment, the localization accuracy improved from a value of 27.7 cm to 6.3 cm, while the RMSE dropped from 0.42 V to 0.20 V.

discrete features in the measured field (e.g., chemical leaks, pollution hot-spots). It implies a threshold segmentation of the measured and reference signals, to define what constitutes a feature (see Figure 11). For a pair of features from the reference signal, s , and the estimated signal, \hat{s} , denoted by their respective areas (or volumes for a 2D signal) A_1 and A_2 , we define the feature localization accuracy metric as the Euclidian distance between the orthogonal projection of their centers of mass (CoMs) on the space axis (or plane for a 2D signal). An investigation of feature discrimination is beyond the purpose of this paper, and consequently we selected a low threshold of 300 mV that yielded a single feature, representative of the entire plume.

- **Root mean squared error (RMSE)** - Differently from the previous metric, the RMSE quantifies the system’s ability to estimate the continuous shape of the underlying signal, and is computed as:

$$RMSE = \sqrt{\frac{1}{N} \sum_k (\hat{s}(k) - s(k))^2} \quad (5)$$

where k represents the discrete space index, and N is the total number of discrete samples.

We performed the same type of experiments with the active sniffer as for the passive set-up: sets of 10 runs for each traversing system movement speed considered. In order to identify the sensor model, the experimental data was divided into model training and evaluation sets, through a leave-one-out cross-validation scheme. Each training set contained measurement data for all of the considered speeds. After training all the models, we applied the Wiener deconvolution to each experimental run, using the model for which the respective data was not included in its training set. Figure 12 shows an example of the signal estimation through

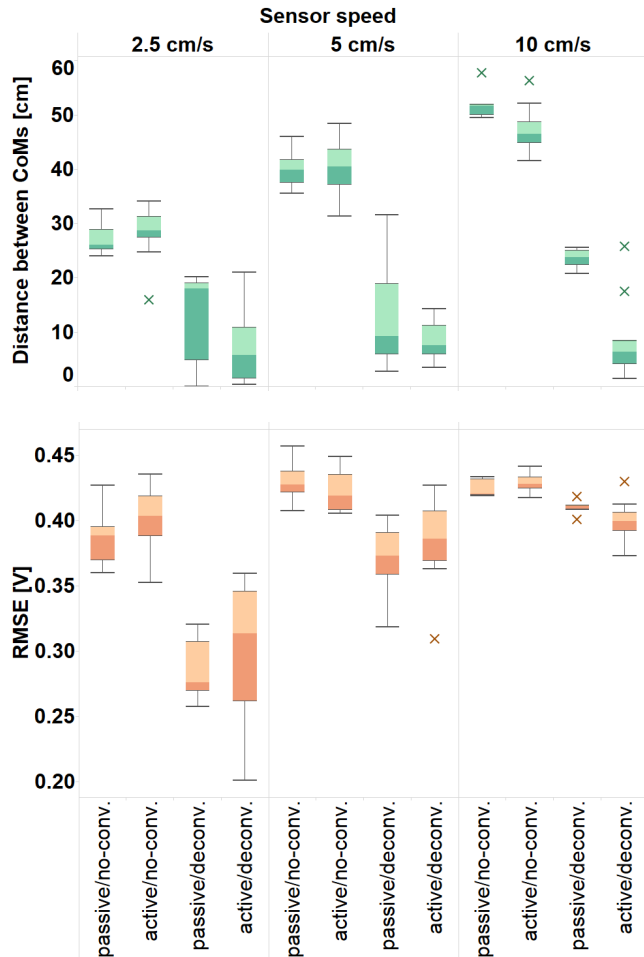


Figure 13. Performance evaluation for each of the considered scenarios: accuracy of feature localization (top), and root mean squared error (bottom).

deconvolution for one of the experiments.

Finally, using the two metrics, we evaluated the performance of the passive and active systems, with and without the Wiener deconvolution, for each experimental run. The results we obtained are presented in Figure 13.

The use of the Wiener deconvolution resulted in consistent performance improvement for all the considered scenarios, and for both metrics. Nevertheless the gain in RMSE quality drops significantly as the movement speed increases. We believe that this is mainly due to the lower signal-to-noise ratio of the more damped signals measured at higher velocities. The feature localization metric does not appear to be affected to the same extent.

The effect of the active sniffer is mostly significant for the feature localization metric, providing a particularly large improvement for the highest speed we considered. In fact, when not used in conjunction with the Wiener deconvolution, no significant advantage can be seen at the lower speeds. Looking at the root mean squared error, no advantage was observed for this active sniffer design.

5 Discussion

The experimental results of this paper show that mobility has a significant effect on the chemical sensor readings. The integrator effect of the slow sensor dynamics was clearly observed at the relatively low movement speeds considered in our experiments, and would certainly be very severe for more realistic mobility speeds. In the future, we plan to get our experimental set-up closer to the mobility conditions experienced in our real-world deployment. In particular, we will be experimenting in a significantly larger testing section of our wind tunnel facilities ($2 \times 4 \times 20 \text{ m}^3$), with a correspondingly larger traversing system, enabling us to increase the sensor mobility.

The results we obtained with our basic active sniffer design were mixed. While it improved the feature localization accuracy, particularly at the highest speed, its impact on the RMSE was not significant. Although it did not deliver the desired performance improvement, experimenting with this simple sniffer enabled us to gain an insight into the non-trivial process of its design. Compared with the passive sampler scenario, the enclosing structure of the sniffer forms a mechanical barrier, which has an important impact on air flow properties around it at different wind and motion speeds (e.g., air turbulence, velocity, density and pressure). The increased performance of the sniffer for the highest considered speed suggests a significantly different flow condition, as the wind angle changes relative to the frame of the sensor node. In this context, the opportunity of using an axial fan for the sniffer needs to be reconsidered. The main advantage of axial fans is their ability to move large volumes of air, but their actual flow rate depends significantly on the background flow conditions. The use of centrifugal fans or positive displacement pumps (e.g., diaphragm pumps) may be an interesting alternative, as they are much less influenced by the background flow. However, they typically supply a significantly lower air throughput.

One of the future research directions we are pursuing is to improve the design of both the shape of the sniffer and its actuation in order to maximize its benefits. We believe that this effort is worthwhile, considering the fact that the ability to produce a higher quality raw measurement signal (i.e. with better signal-to-noise ratio), will be beneficial to any deconvolution technique subsequently applied, allowing for a better signal reconstruction.

Although the Wiener deconvolution consistently produced positive results, there is still room for improvement. One direction that would be useful to investigate is the refinement of the assumed sensor model. One option is the use of a two phase model, with different dynamical properties for the rise and recovery behavior of the sensor, which have been reported to be asymmetrical in previous works [20].

In this work we used the data measured at different sensor movement speeds to derive a single linear model for the distortion of the signal. This is an appropriate approach as long as the distortion is caused exclusively (or predominantly) by the sensor dynamics in conjunction with the platform kinematics. As we plan to expand the range of considered speeds, going towards urban vehicle levels,

we expect that flow perturbation induced by the platform mobility will play a larger role. In this context, a single linear distortion model, independent from platform speed, will probably not be sufficient, and might need to be replaced by either a piece-wise linear model or a nonlinear model.

6 Conclusions

Developing the appropriate techniques for mitigating the effect of slow-dynamics of low-cost chemical sensors is essential for the real-world success of mobile WSNs for air quality monitoring.

In this paper we experimentally analyzed the effect of mobility on readings of a chemical sensor in a controlled environment. Considering three different speeds for the mobile sensor, we showed that the impact of sensor dynamics is not negligible in the experiments. To increase the quality of measurements we proposed and studied two different solutions; (i) using an active sniffing system to augment the flow on the sensor and decrease the sensor response time, and (ii) through a deconvolution technique for reducing the effect of motion blur.

We considered two metrics for evaluation of our proposed techniques; feature localization accuracy and the RMSE. We conclude that the deconvolution process results in consistent performance improvement for all the considered scenarios, and for both metrics. The effect of the active sniffer is mostly significant for the feature localization metric, providing a particularly significant improvement at the highest speed we considered.

7 Acknowledgments

This work was funded by NanoTera.ch, a research initiative scientifically evaluated by the Swiss National Science Foundation and financed by the Swiss Confederation, in the framework of OpenSense II, a follow up on the original OpenSense project.

8 References

- [1] M. Alexandre and M. Gerboles. Review of small commercial sensors for indicative monitoring of ambient gas. *Chemical Engineering Transactions*, 30:169–174, 2012.
- [2] A. Arfire, A. Marjovi, and A. Martinoli. Model-based rendezvous calibration of mobile sensor networks for monitoring air quality. In *Proceedings of the IEEE Sensors Conference 2015*, pages 366–369, 2015.
- [3] E. Bales, N. Nikzad, N. Quick, C. Ziftci, K. Patrick, and W. Griswold. Citisense: Mobile air quality sensing for individuals and communities design and deployment of the citisense mobile air-quality system. In *The 6th International Conference on Pervasive Computing Technologies for Healthcare*, pages 155–158, 2012.
- [4] N. Castell, H.-Y. Liu, M. Kobernus, A. J. Berre, J. Noll, E. Cagatay, and R. Gangdal. Mobile technologies and personalized environmental information for supporting sustainable mobility in Oslo: The citisense-mob approach. In *28th EnviroInfo Conference*, pages 699–706, 2014.
- [5] Centre for Scientific Computing, University of Cambridge. Sensor Networks for Air Quality at Heathrow Airport. <http://www.snaq.org/>. [Online; accessed 25 September 2015].
- [6] Y. Cheng, X. Li, Z. Li, S. Jiang, Y. Li, J. Jia, and X. Jiang. Aircloud: a cloud-based air-quality monitoring system for everyone. In *Proceedings of the 12th ACM Conference on Embedded Network Sensor Systems*, pages 251–265, 2014.
- [7] City Technology Ltd. A3CO Sensor Datasheet. <https://www.citytech.com/PDF-Datasheets/a3co.pdf>. [Online; accessed 26 September 2015].

- [8] P. Dutta, P. M. Aoki, N. Kumar, A. Mainwaring, C. Myers, W. Willett, and A. Woodruff. Common sense: participatory urban sensing using a network of handheld air quality monitors. In *Proceedings of the 7th ACM conference on embedded networked sensor systems*, pages 349–350, 2009.
- [9] B. Elen, J. Peters, M. V. Poppel, N. Bleux, J. Theunis, M. Reggente, and A. Standaert. The aeroflex: a bicycle for mobile air quality measurements. *Sensors*, 13(1):221–240, 2012.
- [10] B. Elen, J. Theunis, S. Ingarra, A. Molino, J. Van den Bossche, M. Reggente, and V. Loreto. The everyaware sensorbox: a tool for community-based air quality monitoring. In *Sensing a Changing World Workshop*, 2012.
- [11] Environmental Protection Agency (EPA). National Ambient Air Quality Standards (NAAQS). <http://www3.epa.gov/ttn/naaqs/criteria.html>. [Online; accessed 29 September 2015].
- [12] European Environment Agency (EEA). Assessment and Management of Urban Air Quality in Europe. http://www.eea.europa.eu/publications/environmental_monograph_2006_5, 1998. [Online; accessed 29 September 2015].
- [13] D. Hasenfratz, O. Saukh, and L. Thiele. On-the-fly calibration of low-cost gas sensors. *Wireless Sensor Networks*, pages 228–244, 2012.
- [14] D. Hasenfratz, O. Saukh, and L. Thiele. Model-driven accuracy bounds for noisy sensor readings. In *9th International Conference on Distributed Computing in Sensor Systems*, pages 165–174, 2013.
- [15] D. Hasenfratz, O. Saukh, C. Walser, C. Hueglin, M. Fierz, T. Arn, J. Beutel, and L. Thiele. Deriving high-resolution urban air pollution maps using mobile sensor nodes. *Pervasive and Mobile Computing*, 16:268–285, 2015.
- [16] W. Hedgecock, P. Völgyesi, A. Ledeczi, X. Koutsoukos, A. Aldroubi, A. Szalay, and A. Terzis. Mobile air pollution monitoring network. In *Proceedings of the 2010 ACM Symposium on Applied Computing*, pages 795–796, 2010.
- [17] Imperial College London. MESSAGE - Mobile Environmental Sensing System Across Grid Environments. <http://www3.imperial.ac.uk/lesc/projects/archived/mobileenviron>. [Online; accessed 25 September 2015].
- [18] A. Kohnotoh and H. Ishida. Active stereo olfactory sensing system for localization of gas/odor source. In *7th International Conference on Machine Learning and Applications*, pages 476–481, 2008.
- [19] J. J. Li, A. Jutzeler, and B. Faltings. Estimating urban ultrafine particle distributions with gaussian process models. In *S. Winter and C. Rizos (Eds.): Research@ Locate14*, pages 145–153, 2014.
- [20] A. Lilienthal and T. Duckett. A stereo electronic nose for a mobile inspection robot. In *1st International Workshop on Robotic Sensing*, 2003.
- [21] A. Lilienthal and T. Duckett. Building gas concentration gridmaps with a mobile robot. *Robotics and Autonomous Systems*, 48(1):3–16, 2004.
- [22] T. Lochmatter and A. Martinoli. Tracking an odor plume in a laminar wind field with the crosswind-surge algorithm. In *Proc. of the Eleventh Int. Symp. Experimental Robotics*, volume 54, pages 473–482, 2008.
- [23] A. Marjovi, A. Arfire, and A. Martinoli. High resolution air pollution maps in urban environments using mobile sensor networks. In *11th International Conference on Distributed Computing in Sensor Systems*, pages 11–20, 2015.
- [24] Pea Soup Ltd. Wind Tunnel Air Flow Tracer Brochure. <http://www.smokemachines.net/PDF/Air-flow-tracer-brochure.pdf>. [Online; accessed 26 September 2015].
- [25] Preemptive Media. AIR - Area’s Immediate Reading. <http://www.pm-air.net/index.php>. [Online; accessed 25 September 2015].
- [26] O. Saukh, D. Hasenfratz, and L. Thiele. Reducing multi-hop calibration errors in large-scale mobile sensor networks. In *14th International Conference on Information Processing in Sensor Networks*, pages 274–285, Seattle, WA, USA, Apr 2015.
- [27] O. Saukh, D. Hasenfratz, C. Walser, and L. Thiele. On rendezvous in mobile sensing networks. In *Real-World Wireless Sensor Networks*, pages 29–42, 2014.
- [28] SENSEable City Laboratory, MIT. The Copenhagen Wheel. <http://senseable.mit.edu/copenhagenwheel/>. [Online; accessed 25 September 2015].
- [29] E. G. Snyder, T. H. Watkins, P. A. Solomon, E. D. Thoma, R. W. Williams, G. S. Hagler, D. Shelow, D. A. Hindin, V. J. Kilaru, and P. W. Preuss. The changing paradigm of air pollution monitoring. *Environmental Science & Technology*, 47(20):11369–11377, 2013.
- [30] C. Stachniss, C. Plagemann, A. J. Lilienthal, and W. Burgard. Gas distribution modeling using sparse gaussian process mixture models. In *Robotics: Science and Systems IV*, pages 310–317, 2009.
- [31] World Health Organization (WHO). News release, 25 March 2014, Geneva. <http://www.who.int/mediacentre/news/releases/2014/air-pollution/en/>. [Online; accessed 25 September 2015].